Proceedings of 2001 Korea-Japan Joint Seminar
on Particle Image Velocimetry
Seoul National Univ., Dec. 3 - 4

Flow Characteristics of Liquid Ramjet Engines using Two Color PIV

Kyubok Ahn and Youngbin Yoon

School of Mechanical and Aerospace Engineering, Seoul National University,
Seoul, KOREA, 151-742

Abstract A two color PIV technique has been developed for visualization of complex and high speed flow in a ramjet combustor. Two color PIV has the advantages that velocity distributions in high speed flowfields can be measured simply by varying the time interval between two different laser beams and a directional ambiguity problem can be solved by color separation, and then a signal-to-noise ratio can be increased through nearly perfect cross-correlation. As a basic research of the ramjet engine, a 2-D shaped combustor with two symmetric air intakes has been manufactured and an experimental study has been conducted using a two color PIV technique. The flow characteristics such as recirculation zones, intake air mixing and turbulent kinetic energy have been investigated varying inlet angles and dome heights. It was found that the primary recirculation zone is affected mainly by the dome height, whereas the secondary recirculation zone is influenced by the air inlet angle.

1. Introduction

In conventional air-breathing jet engines, air has to be compressed before entering into a combustor to improve the efficiency. Thus, there are multi-compressor and turbine in turbo jet engines. However, in supersonic speed (Mach>2), sufficient compression ratio can be obtained without compressor from the ram effect that the air pressure becomes higher through the shockwaves by passing supersonic inlets. The ramjet engine takes advantage of this effect [1]. Ramjet engine doesn't need complex compressor and turbine to run compressor, and thus the structure is very simple and it has good efficiency in supersonic region.

In general, most of missiles use rocket engines. However, since rocket engines must be equipped with extra oxidizer, its payload is 10 % of total weight at most. Specific impulse is also considerably low. Hence, in order to obtain higher efficiency it has been considered to change to air-breathing propulsion system in missiles. The performance of attack and defense system that is being developed very rapidly requires high performance engines. Although ramjet engines can't take a static thrust so that they needs auxiliary boosters, they perform about four times higher compared with existing rocket engines and are suitable for supersonic and long distance flight requirements. Therefore, many advanced countries have an interest in ramjet engines [2].

Static thrust which is the most crucial problem of ramjet engines was resolved by a device such as CRJ(Conventional can combustor Ramjet), ATRJ(Air-Turbo Ramjet), ERJ(Ejector Ramjet), IRR(Integral Rocket Ramjet), ADR(Air Ducted Ramjet). Particularly, sufficient progress was accomplished by ADR, IRR in aspect of the volume or weight [3-4].

Also, the design of ramjet combustor is critical part because the combustion efficiency of ramjet is strongly dependent upon the combustor geometry. In liquid ramjet engines, liquid fuel is injected upstream of combustor and mixed with intake air. And then, ignition occurs at the recirculation zone, which behaves as a flame holder. Thus, flame stabilization must be provided by the existence of the proper size of recirculation zones in ramjet combustors. Previously, many techniques, such as surface oil flow technique [5], surface flow visualization [6], static pressure and five-hole pitot probe [7] and so on, were applied to measurement of recirculation zone in ramjet combustors.

In the present study, flow characteristics in the axisymmetric liquid ramjet combustor have been observed using 2-color PIV by varying inflow angles and dome heights. From result of velocity fields, recirculation zone, vorticity fields, turbulence strength, and mixing characteristics have been analyzed.

2. Experimental Apparatus

1) The Ramjet Engine Combustor

Figure 1 shows the schematic of the ramjet system which consists of a ring blower for producing air, a settling chamber for stabilizing air, an aerosol generator for flow visualization and a 2-D shaped combustor with two symmetric air intakes. For direct connect test without air inlet, a ring blower is used to supply air flow of maximum 8 m^3/min and a setting chamber is used to stabilize air supplied by a blower. And then, SiO_2 particles are seeded into a settling chamber by a funnel type aerosol generator for flow visualization. Particle seeding density is controlled by a regulator, which is connected to a compressor. The stabilized air in a settling chamber is separated into two combustor inlet ducts for controlling air flow of two inlet ducts according to flight conditions. And an air mass flux in a combustor inlet duct is controlled precisely through a valve. The air flow of an inlet duct goes through an orifice, which is built to measure mass flux, and is supplied into a model combustor.

The model combustor of the ramjet system is shown in Fig. 2. The dome height (h_D) has been varied as 12.5, 22.5, 32.5 and 42.5 mm from a combustor inlet for investigating the effect of dome height. A dome is composed of two parts to enable laser sheet beam to pass the centerline of a dome and go through a combustor. The size of a model combustor is 50 × 50 × 280 mm (H × W × L). A quartz window is built in the wall of dome to pass laser sheet beam for flow visualization and measuring the velocity, and visualization windows are built in the side walls of the combustor for taking images. The combustor inlets are symmetric and have been varied with different angles of 45°, 60° and 90° for investigating the effect of inlet angle.

As mentioned previously, the model combustor is manufactured to study the flow characteristics of ramjet combustor according to combustor geometries such as combustor inlet angle and combustor dome height as shown in Fig. 3. All measurements are performed on the central plane of the two-dimensional model.

2) Two Color PIV System

Figure 4 shows the schematic of the two color PIV system. In this experiment, a green color laser beam (532nm: 2nd harmonic beam of YAG laser) and a red color laser beam (619nm: output beam from YAG pumped Dye laser) are combined by a dichroic beam combiner mirror and directed through cylindrical lens and spherical lens to make sheet beams. Since the divergence of two laser beams is different, two convex lenses are used to focus two laser beams at the same location. The power of laser is 30 mJ/pulse and the pulse duration of each laser pulse is 8 ns. The pulse separation between two laser beams is controlled by a delay generator (Stanford, DG535). The pulse separation is confirmed using a photo-diode and is fixed to 7 μs, that is equivalent to a particle image displacement of 20 % of the interrogation region length.

Scattered images from seeding particles are recorded on a high resolution (3060 × 2036) Kodak digital CCD camera (DCS 460) equipped with f/2.8 AF Micro Nikkor 105 mm lens. The F-number of 105 mm lens is fixed to 4.0 in the present experiments. The opening time of the camera shutter is controlled by another delay generator for the synchronization with laser pulses. In the present research, all PIV components are synchronized using the delay generators (Stanford, DG535).

3. Two Color PIV Technique

1) Principle of Two Color PIV

Two color PIV technique can be one of methods to solve the directional ambiguity problem related to auto-correlation and was performed for the first time by Goss et al.[8]. Although two color PIV is based on single-frame/double-exposure, this single frame can be divided into two frames by color separation, which have different color image as shown in Fig. 5. Therefore, nearly perfect cross-correlation process can be used and thus high signal-to-noise ratio can be obtained and dynamic range can be increased. Also the application to high speed flows such as supersonic flows can be possible since the pulse separation between two laser beams can be controlled below μs.

The present cross-correlation technique is based on intensity maps of the red and green images of the scattered light. Considering the intensity distribution of red and green images r(x, y) and g(x, y), and their corresponding Fourier transforms R(a, b) and G(a, b), the two-dimensional cross-correlation function

$$h(x,y) = \int_R \int_R r(a,b)g(x+a,y+b)dadb$$
$$= \mathrm{F}^{-1}\left[\mathrm{F}(\mathrm{r}(\mathrm{x},\mathrm{y}))\,\mathrm{F}(\mathrm{g}^*(\mathrm{x},\mathrm{y}))\right]$$
$$= \mathrm{F}^{-1}\left[\mathrm{R}(\mathrm{a},\mathrm{b})\,\mathrm{G}^*(\mathrm{a},\mathrm{b})\right]$$

is employed to determine the magnitude and direction of the average velocity over the interrogation area.

The correlation function is calculated over interrogation domains of the PIV image. The size of interrogation domains depends on the particle density, local velocity gradients, particle image size and the desired spatial resolution. In present research, the interrogation domain measured 64 × 64 pixels

corresponding to 3.5 × 3.5 mm in the measured flow. In order to enhance the overall resolution, the interrogation domains are overlapped by one-half the domain size. And an intensity weighted peak searching algorithm is used to determine the exact location of the peak with a sub-pixel accuracy. In the post processing, a median filter is used to remove some bad vectors.

2) Image Processing of Two Color PIV

In early experimental approaches involving the PIV technique, the particle images were recorded on photographic films. However, this type of recording is time consuming due to wet processing of the films before digitization and subsequent computer processing. This disadvantage can be overcome by recording the particle images directly onto a two-dimensional CCD array. In present research, a high resolution digital (3060 × 2036) color CCD camera (Kodak, DCS460) is used to eliminate the processing time and subsequent digitization time of color film and the complexities associated with conventional image-shifting technique.

The Kodak Model DCS 460 color camera utilizes a single large-scale CCD sensor to record color images. Each camera element (pixel) is coated with either a red, green, or blue color filter (Fig. 6). Because the green color yields the best measure of brightness to the human eye, the green pixels are composed of 50 % of the camera sensor. The remaining pixels are equally divided between red and blue elements. Achieving a full 3060 × 2036 RGB TIFF image requires a multi-step process; i.e., red, green, and blue pixels are interpolated during this process. The software to expand the captured compressed CCD image into a full RGB TIFF image is supplied by Kodak as a plug-in for the image processing package Adobe Photoshop.

In interpolation processing, the green components of non-green pixels for the first and last two columns of the camera are assigned values of the adjacent green pixels. The green components of the non-green pixels of the remaining image are assigned the average values of the closest surrounding green pixels. The green pixels used in this average are selected on the basis of the brightness of the surrounding red and blue pixels. Once the green interpolated image has been constructed, the remaining red and blue image interpolations can take place. In the red-image interpolation, the first two columns are unique. Red pixels retain their original values, while red components of green and blue pixels are assigned to the average value of adjacent red pixels minus their green components. In addition, the green component of the non-red pixel is added to the average value to retain luminance. The same procedure is used for the blue pixels. However, this provided procedure of image processing may not be adequate for obtaining raw color images although this may produce the natural color images of the objects. Consequently, this procedure may result in erroneous images to obtain accurate velocity fields using PIV. Thus, in-house decompression software was developed to reduce the bad vector rates and improve the accuracy of velocity vectors after confirming with known velocity field using LDV. Figure 6 shows the interpolation process of in-house software.

4. Results and Discussion

1) Characteristics of Velocity Fields and Recirculation Zones

The velocity of air entering into the ramjet combustor is approximately Mach 0.3, which is larger than the velocity of flame propagation. Thus, it is required to have flame holder for flame stabilization. In the present study, a side dump ramjet combustor is used for flame holding. Generally, it is known that primary recirculation zones is found between a dome and a combustor inlet, and second recirculation zones is generated near the wall behind a combustor inlet as shown in Fig. 7. The inlet air flow is fixed to 88 m/s which is corresponding to Re = $O(10^5)$ and Ma $\fallingdotseq$ 0.3 based on the inlet width (16mm). The velocity vectors are obtained for all cases of 3 inlet angles and 4 dome heights.

Figure 7 shows the 66% skipped vector map from the full vector map with the variation of dome height at inlet angle of 45°. From the results of velocity fields, streamlines, vorticity fields and turbulent intensity fields are obtained for analyzing the flow characteristics. It is found that the well-defined reverse flow regions are found near the dome and the walls. The position of zero velocity gives an approximate location of the core of the wall recirculation zones. As the size of dome height increases, the size of primary recirculation is increased. Also, as the inlet air enters the combustor, the individual peak location of the two jets from each inlet merges together downstream of combustor due to mixing. Finally, the two jets merge near the centerline, and then the flow develops to a bell-shaped velocity profile, which indicates that the flow approaches a fully developed flow condition. And high vorticity zones are observed near the boundaries of primary and secondary recirculation zones.

The axial component (U) of the centerline velocity is shown in Fig. 9 as functions of dome heights and inlet angles. It is noted that U profiles are almost same trend regardless of different dome heights as shown in Fig. 9 (a). At fixed θ of 60°, the values of U are small inside primary recirculation zone but show negative near the impinging regions near the inlets ($0<x/H<0.5$). However, U component increases and shows a maximum near x/H=1.2, which is greater than 60m/s and then decreases downstream of the combustor. On the contrary, U profiles show different trends at different inlet angles as shown in Fig. 9(b). As an inlet angle increases, the maximum peak location of the centerline velocity decreases into smaller x/H. Hence, it is expected that as an inlet angle increases the flow attains uniform velocity conditions earlier; i.e., in case of $\theta = 90°$, more intense mixing can be expected in the initial regions and the uniform flow conditions can be achieved earlier than for smaller angles. For example, the peak value of velocity at the centerline occurs at x/H = 1.2 for $\theta = 60°$ and at x/H = 0.8 for $\theta = 90°$, which indicates the location of the merging point of the two jets. Beyond these x/H values, the non-uniformity in the profiles decreases due to the mixing of the flows and eventually they become nearly uniform.

Figure 10 shows the effect of dome height on the primary and secondary recirculation zones at inlet angle of 45°. As the dome height increases, the size of primary recirculation zone is increased linearly whereas the size of secondary recirculation zone shows a maximum at h_D = 22.5 mm. The height and width in Fig. 10 indicate the values of secondary recirculation zone. Thus, the reduction of secondary recirculation size is believed to be due to the reduction of width as the dome height increases. In summary,

it is found that the dome height influences the primary recirculation zone mainly rather than the secondary recircualton zone. Hence, it is recommended that the optimum value of dome height is determined from the trend of secondary recircualtion zone.

Figure 11 shows the velocity, streamlines and vorticity fields at $h_D/H = 0.45$ with inlet angle varied. As shown in Fig. 11(b), the secondary recirculation zone is substantially influenced by the inlet air angle; as the inlet angle increases, the height and width of secondary recirculation zone are increased. On the contrary, the primary recirculation zone is slightly affected by the inlet angle; the width of primary recirculation zone is reduced as the inlet angle increases. At $\theta = 90°$, the impinging momentum from two inlets should be largest so that the mixing rate is expected to be maximized. However, the primary recirculation zone is reduced by more than one half. Figure 12 shows the trends of recirculation size variation with respect to the inlet angle at $h_D/H = 0.25$. Although the condition of Fig. 12 is different from Fig. 11, the general trends obtained by the variation of inlet angle are shown to be very similar.

2) Turbulence Characteristics

From the measured values of the turbulent components, the mean turbulent kinetic energy (q^2) is obtained. The variation of q^2 is presented in Fig. 13, where q^2 is normalized by U_o^2. Since U_o^2 is a measure of the inlet total kinetic energy, q^2/U_o^2 represents a fraction of the total inlet kinetic energy converted to turbulence. It is interesting to observe the influence of the primary and secondary recirculation zones on the distribution of the total turbulent kinetic energy. From Fig. 18, it is expected that the high levels of q^2 in the core flow are due to the influence of the shear layers associated with the second recirculation zone which act as regions of production of turbulent kinetic energy. The turbulence that is produced at the shear layer near the second recirculation zone is diffusing towards the centerline and this, coupled with the decay of mean velocity in this region, gives rise to the increase of turbulence intensity at the centerline. The turbulence being generated in the initial region is dissipated in the downstream region. Comparing the distribution of turbulent kinetic energy along the centerline with those of the mean velocity, it could be inferred that the turbulent kinetic energy increases in the region corresponding to steep mean velocity gradients.

5. Summary

The flow characteristics of the model ramjet combustor at atmospheric pressure and temperature conditions have been analyzed with two color PIV technique. The major consideration of ramjet combustor design is the stabilization of flames, which is provided by the size of recirculation zones : primary and secondary recirculation zones which are classified by the its locations.

Results show that the primary and secondary recirculation zones are greatly influenced by the inlet angle and dome height. The inlet angle affects the secondary recirculation zone significantly, whereas the dome height influences the primary recirculation zone. Also, the mixing rate of two air streams can be expected by the location of maximum axial velocity component. This is related to the impinging momentum of inlet air or the inlet air angle.

6. References

[1] Hill, P. G. and Peterson, C., Mechanics and Thermodynamics of Propulsion 2nd Ed., Addsion-Wesley Publishing Company, 1992.

[2] Kim, Y. G. ,Kim, K. M. , "Ramjet Technology and Its Development Trends", Journal of The Korean Society for Aeronautical and Space Sciences, Vol. 23, No. 5, pp. 171 – 182, 1995.

[3] Waltrup, P. J., White, M. E., Zarlingo, F. and Gravlin, E. S., "History of U.S. Navy Ramjet, Scramjet and Mixed-cycle Propulsion Development", AIAA Publisher, 1996.

[4] Wilson, R., Limage, C. and Hewitt, P., "The Evolution of Ramjet Missile Propulsion in the U.S. and Where We Are Headed", AIAA Publisher, 1996.

[5] Drewry, J. E. , "Fluid Dynamic characterization of Sudden-Expansion Ramjet Combustor Flowfields", AIAA Journal, Vol. 16, No. 4, pp. 313-319, 1978.

[6] Chittilapilly, L. T., Venkateswaran, S. , Paul, P. J. and Mukunda, H. S., "Flow Measurements in a Model Ramjet Secondary Combustion Chamber", J. Propulsion, Vol. 6, pp. 727-731, 1990.

[7] Manjunath, A., Gowda, B. H. L. and Natarajan, R., "Studies on the mixing of two non-axial plane jets in a confined passage: mean flow characteristics", Experiments in Fluids, Vol. 11, pp 17-24, 1991.

[8] Goss, L. P., Post, M. E., Trump, D. D. and Sarka, B., "Two-color particle-image velocimetry", J. Laser Appl., Vol. 3, pp.36-42, 1991.

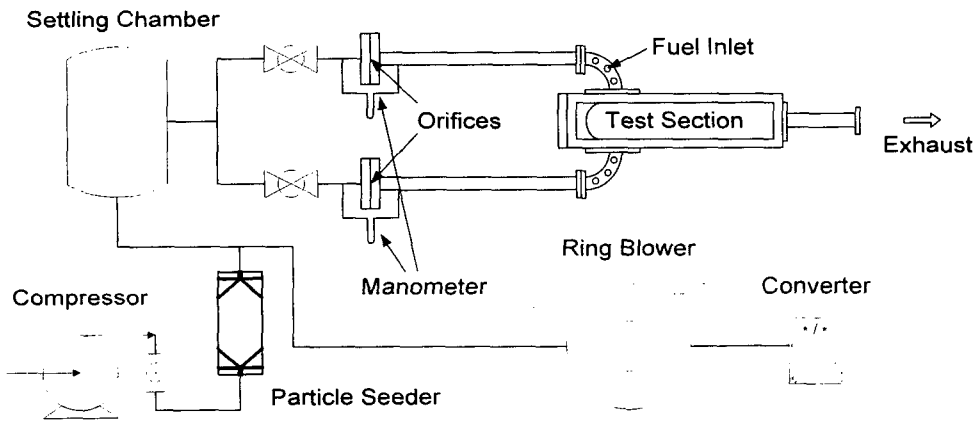

Fig. 1 Schematic of the ramjet system

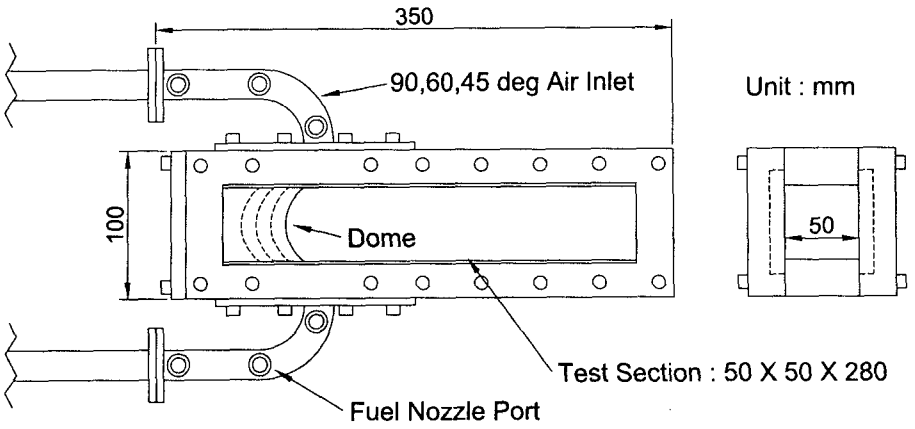

Fig. 2 Schematic of the model ramjet combustor

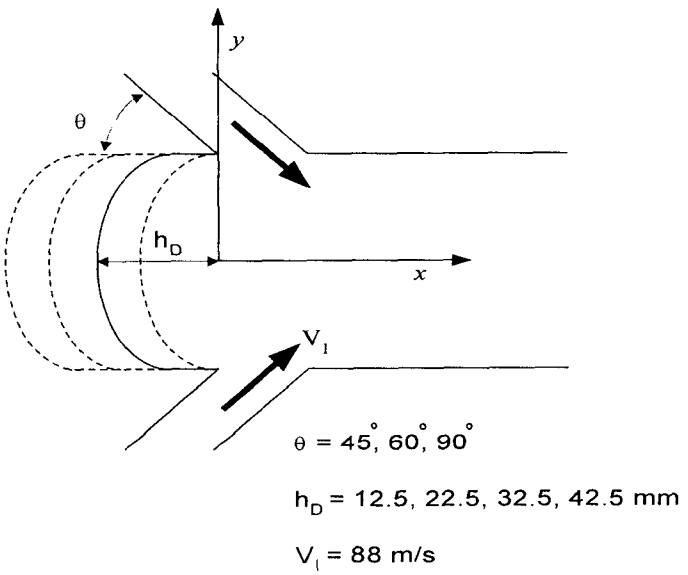

Fig. 3 Experimental conditions of the model ramjet combustor

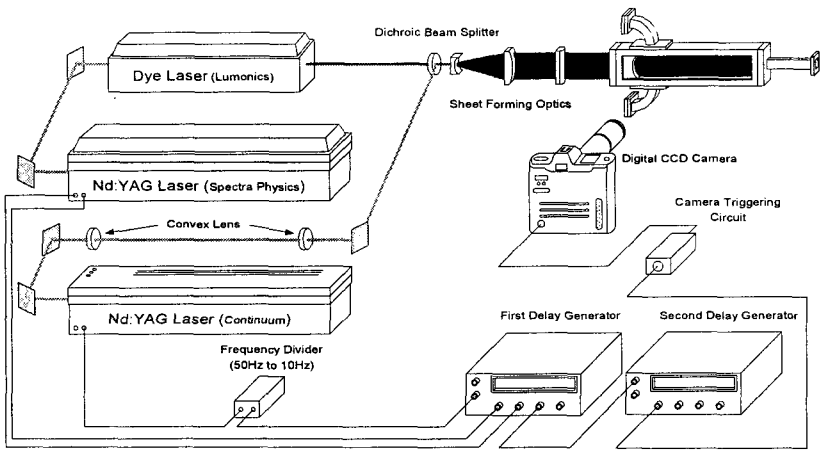

Fig. 4 Two color PIV system

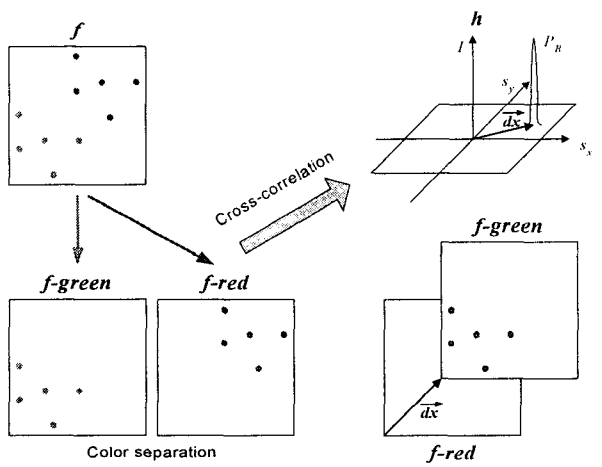

Fig. 5 Cross-correlation procedure of two color PIV

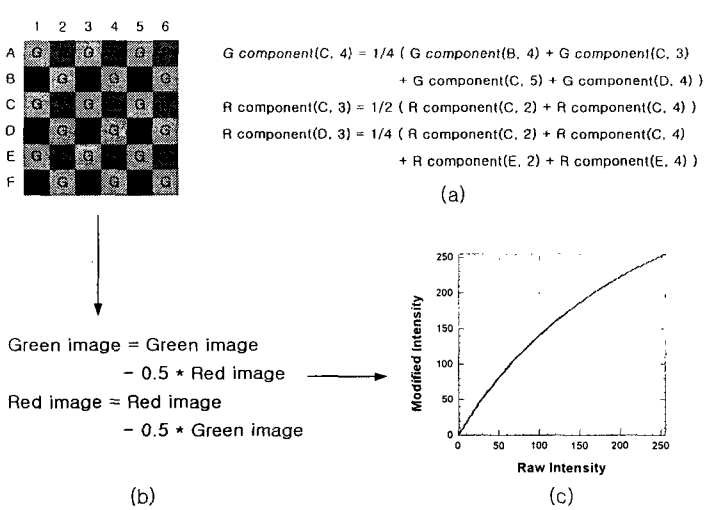

Fig. 6 Decompression process

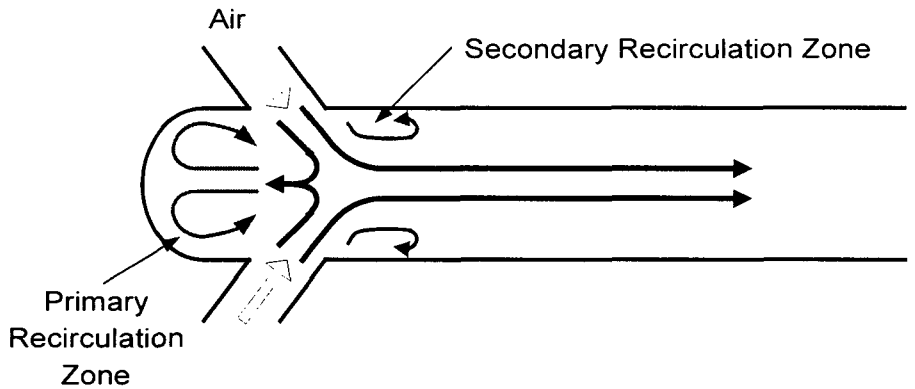

Fig. 7 Schematic of recirculation zones in the ramjet combustor

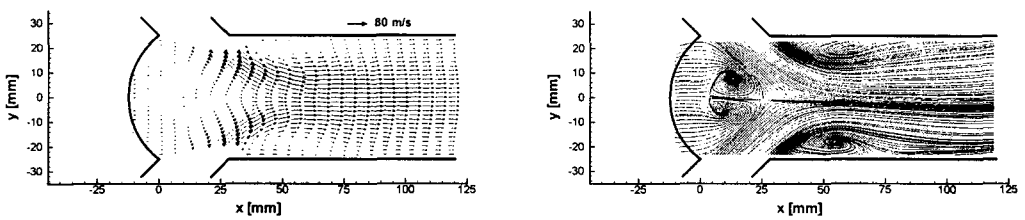

(a) $h_D/H = 0.25$

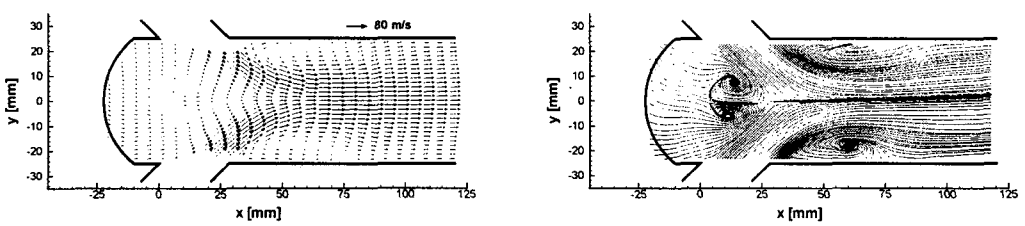

(b) $h_D/H = 0.45$

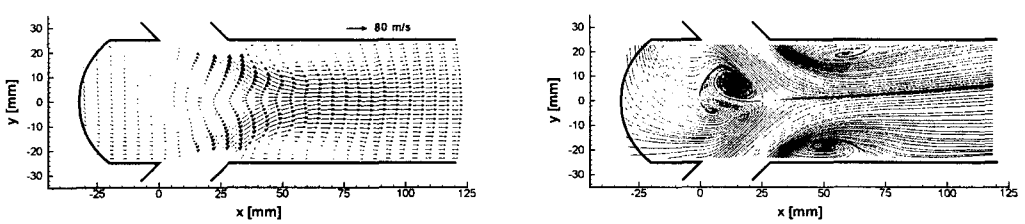

(c) $h_D/H = 0.65$

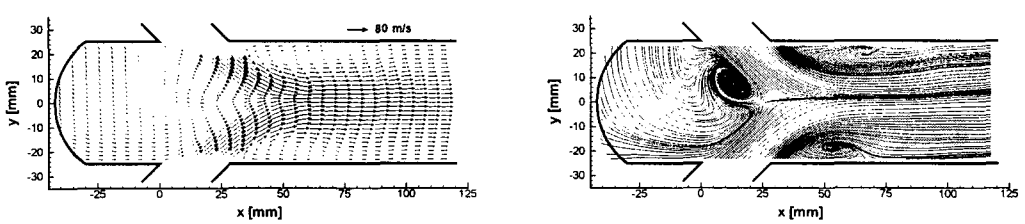

(d) $h_D/H = 0.85$

Fig. 8 Flow fields in the model ramjet combustor at $\theta = 45°$; left figures show velocity fields, right figures show stream lines and vorticity fields.

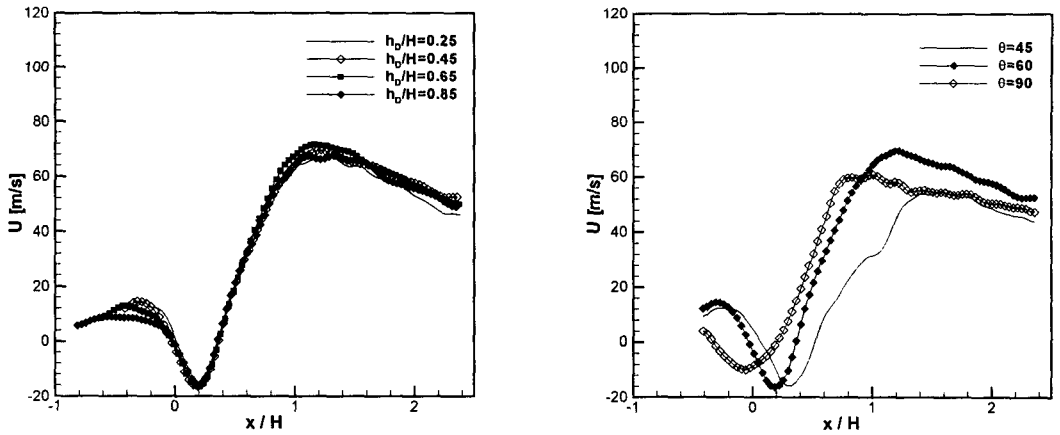

(a) (b)

Fig. 9 Axial component (U) of centerline velocity with inlet angle and dome height varied
(a) θ = 60° with various dome heights (b) h_D/H = 0.45 with various inlet angles

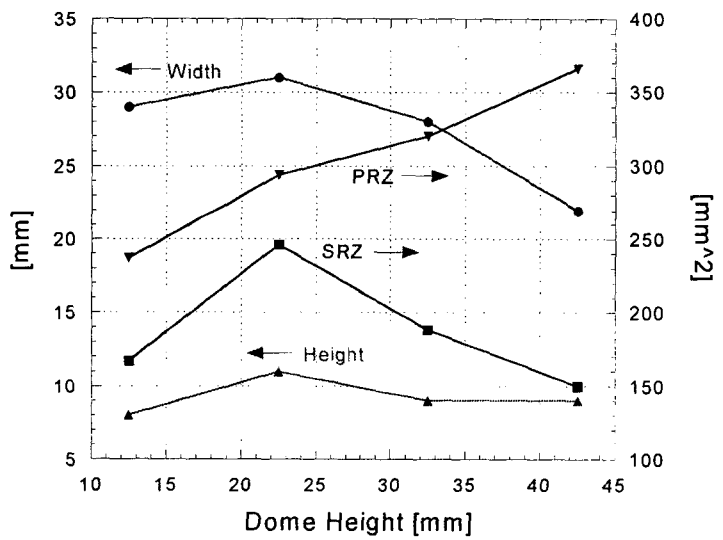

Fig. 10 Effect of dome height on recirculation zone at θ = 45°

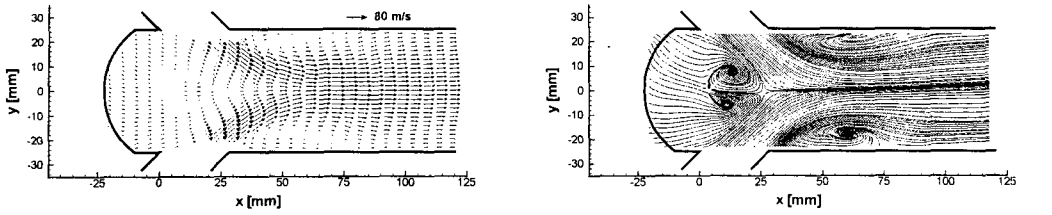

(a) $\theta = 45°$

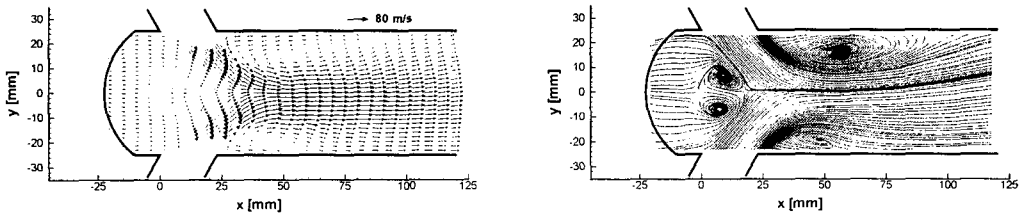

(b) $\theta = 60°$

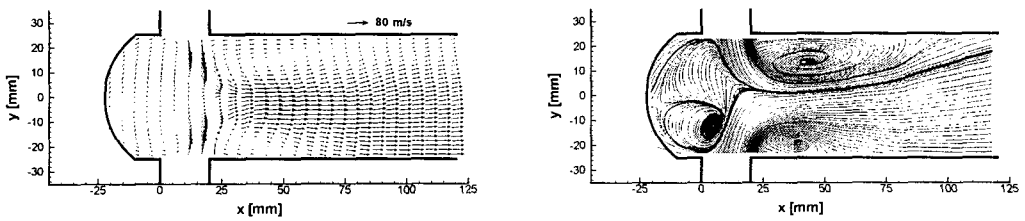

(c) $\theta = 90°$

(d)

Fig. 11 Flow fields in the model ramjet combustor at $h_D/H = 0.45$; left figures show velocity fields, right figures show stream lines and vorticity fields.

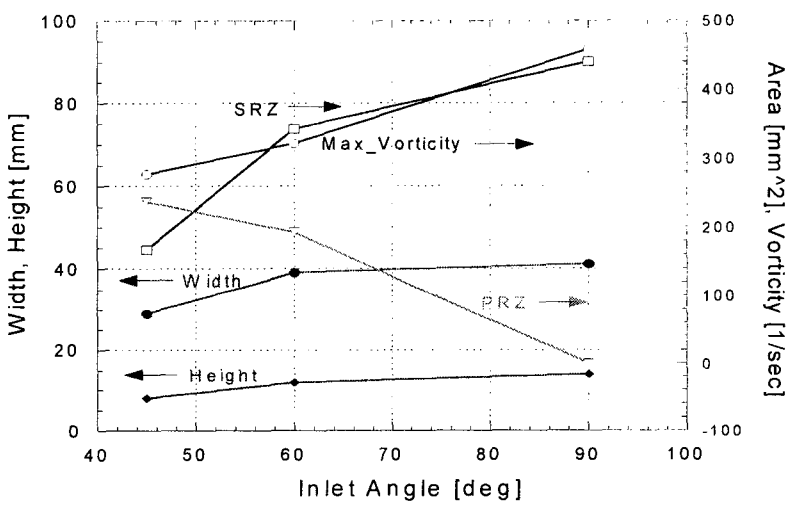

Fig. 12 Effect of inlet angle on recirculation zones at $h_D/H = 0.25$.

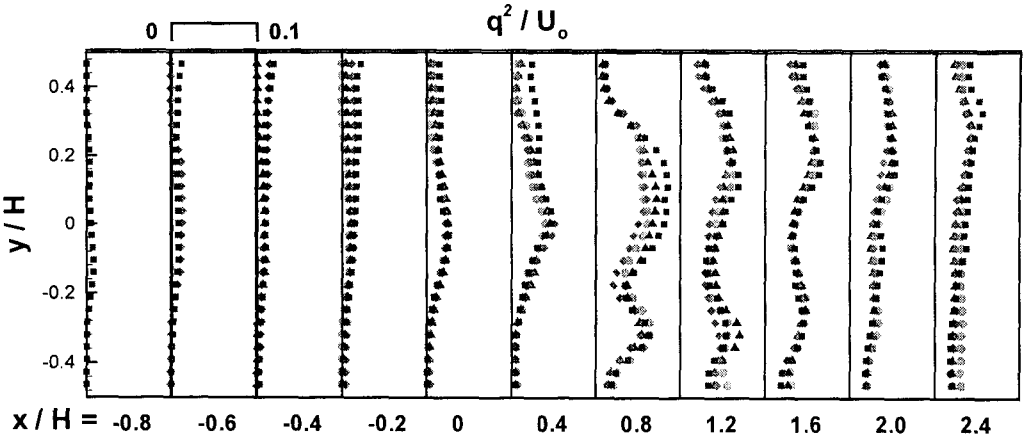

Fig. 13 Distribution of tubulent kinetic energy at $\theta = 60°$